

**$^{55}\text{Mn}$  NMR study of the electron-doped manganite  $\text{Bi}_{0.125}\text{Ca}_{0.875}\text{MnO}_3$** 

Kenji Shimizu\*

*Faculty of Education, Toyama University, Toyama 930-8555, Japan*

Y. Qin and T. A. Tyson

*Department of Physics, New Jersey Institute of Technology, Newark, New Jersey 07102, USA*

(Received 2 July 2005; revised manuscript received 17 April 2006; published 18 May 2006)

We have carried out  $^{55}\text{Mn}$  NMR measurements on  $\text{Bi}_{0.125}\text{Ca}_{0.875}\text{MnO}_3$  and  $\text{CaMnO}_3$ . NMR signals have been observed for  $\text{Bi}_{0.125}\text{Ca}_{0.875}\text{MnO}_3$  at 4.2 K around 100 MHz, 320 MHz, and 605 MHz. The lines around 100 MHz and 605 MHz are ascribed to regions with ferromagnetic spin structure from their behavior in external magnetic fields. The main resonance line observed around 320 MHz has two peaks at 298 and 318 MHz at 4.2 K. The magnetic field dependence of the lines up to 4 T show that they originate from regions with antiferromagnetic spin structure. This is consistent with the observed lack of saturation of the magnetization at high magnetic fields.

DOI: 10.1103/PhysRevB.73.174420

PACS number(s): 76.60.-k, 75.47.Lx, 75.30.Kz

**I. INTRODUCTION**

The electric and magnetic properties of  $\text{Bi}_{1-x}\text{Ca}_x\text{MnO}_3$  have received considerable attention in recent years.<sup>1-5</sup> The end member of the system,  $\text{BiMnO}_3$  is of an insulating ferromagnetic (FM) state at low temperature,<sup>6</sup> although the typical perovskite manganite,  $\text{LaMnO}_3$ , in which the ionic radius of  $\text{La}^{3+}$  is similar to that of  $\text{Bi}^{3+}$ , is the *A*-type antiferromagnetic (AFM) insulator.<sup>7</sup> The insulating FM state has been explained by a lone pair  $6s^2$  electrons.<sup>6,8</sup>  $\text{BiMnO}_3$  is a candidate for multiferroic materials, i.e., both ferromagnetic and ferroelectric states occur simultaneously in the same phase.<sup>9,10</sup> The other end member,  $\text{CaMnO}_3$ , is the *G*-type antiferromagnet.<sup>7</sup> The system,  $\text{Bi}_{1-x}\text{Ca}_x\text{MnO}_3$ , is insulating over a broad compositional range.<sup>5</sup> In addition, a charge ordered AFM structure has also been observed over the wide compositional range. Long period structures associated with charge ordering have been observed in  $\text{Bi}_{0.2}\text{Ca}_{0.8}\text{MnO}_3$ .<sup>11</sup> A ferromagnetic state has been observed in a small range around  $x \sim 0.12$ , where the resistivity is small, e.g., as low as  $10^{-2} \Omega \text{ cm}$  in  $\text{Bi}_{0.125}\text{Ca}_{0.875}\text{MnO}_3$ . However, the temperature dependence of resistivity shows a semiconductinglike behavior, i.e.,  $d\rho/dT < 0$ . Furthermore, the saturation magnetization of  $\text{Bi}_{0.125}\text{Ca}_{0.875}\text{MnO}_3$  is about 1/3 of the fully aligned value of  $3.1 \mu_B/\text{Mn}$ ,<sup>1</sup> which suggests a canted AFM phase or a phase separation into an AFM phase and a FM phase. A recent theoretical treatment of a canted spin ground state proposed that the homogeneous canted spin state seems to be nearly unstable, and tends to phase separate into a mixture of the antiferromagnetic state and ferromagnetic/canted state.<sup>12</sup> In fact, the phase separation into the *G*-type AFM and the *C*-type AFM has been found around  $x \sim 0.12$  in the electron-doped manganites  $R_x\text{Ca}_{1-x}\text{MnO}_3$  ( $R = \text{La, Ce, Sm, Bi}$ ).<sup>4,13-15</sup>

In this paper, we report  $^{55}\text{Mn}$  results of  $\text{Bi}_{0.125}\text{Ca}_{0.875}\text{MnO}_3$  and  $\text{CaMnO}_3$ , using spin-echo NMR technique. In magnetically ordered mixed valence manganites, the magnetic hyperfine field,  $\mathbf{H}_{\text{hf}}$ , mainly arises from the Fermi contact interaction due to the core polarization, and is antiparallel to the spin magnetic moment. Then,  $\mathbf{H}_{\text{hf}}$  is written by  $\mathbf{H}_{\text{hf}} = -\frac{2\pi}{\gamma h} \mathbf{A} \langle \mathbf{S} \rangle$ , where  $\mathbf{A}$  is the hyperfine coupling ten-

sor, and  $\langle \mathbf{S} \rangle$  is the average value of the electron spin proportional to spontaneous magnetization. When applying an external magnetic field  $\mathbf{H}_0$ , the NMR frequency,  $\nu$ , is given by

$$\nu = \frac{\gamma}{2\pi} |\mathbf{H}_0 + \mathbf{H}_{\text{hf}}|. \quad (1)$$

In  $R_{1-x}A_x\text{MnO}_3$  ( $R$ , rare-earth;  $A$ , alkaline-earth) ferromagnetic perovskite manganites, the NMR spectrum arising from  $\text{Mn}^{3+}$  at low temperature falls into the frequency range 350–435 MHz,<sup>16</sup> and that from  $\text{Mn}^{4+}$  is rather narrow and symmetric, compared to that of  $\text{Mn}^{3+}$ , and is observed around 320 MHz, depending on both the substitution element  $A$  and the composition.<sup>16-19</sup>

**II. EXPERIMENTAL DETAILS**

Polycrystalline samples used in the present study were synthesized by a standard ceramic technique. Stoichiometric mixtures of  $\text{Bi}_2\text{O}_3$ ,  $\text{CaCO}_3$ , and  $\text{MnO}_2$  were ground and pressed into pellets. They were calcined at 1000 °C in air for 5 hours then cooled at a rate of 2 °C/min. Then, the samples were reground and sintered at 1200 °C in air for 5 hours then cooled at a rate of 5 °C/min. This procedure was repeated three times.

NMR measurements were carried out using a home-built coherent spin-echo apparatus. NMR spectra were obtained by measuring the integrated spin-echo signal versus frequency. A typical spin-echo sequence of  $0.2-\tau-0.2 \mu\text{s}$  with  $\tau=3 \mu\text{s}$  was used for zero external magnetic field, and  $1-\tau-2 \mu\text{s}$  with  $\tau=5 \mu\text{s}$  for measurements in external magnetic fields.

**III. RESULTS AND DISCUSSION**

Figure 1 shows the NMR spectrum of  $^{55}\text{Mn}$  in  $\text{Bi}_{0.125}\text{Ca}_{0.875}\text{MnO}_3$  at 4.2 K in zero external magnetic field. NMR signals have been observed at around 100, 320, and 605 MHz. The NMR spectrum for  $\text{CaMnO}_3$  is also shown in

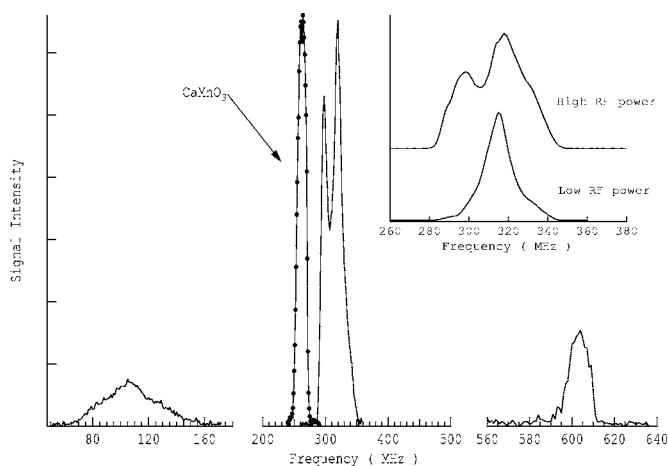


FIG. 1. Zero-field  $^{55}\text{Mn}$  NMR spectra for  $\text{Bi}_{0.125}\text{Ca}_{0.875}\text{MnO}_3$  and  $\text{CaMnO}_3$  taken at 4.2 K. The inset shows the rf field dependence of line shape of  $\text{Bi}_{0.125}\text{Ca}_{0.875}\text{MnO}_3$ .

the figure. It is surprising that NMR signals are observed in the low frequency range 60–160 MHz for mixed valence perovskite manganites. The line at 605 MHz may be attributed to  $\text{Mn}^{2+}$ . The line around 600 MHz has been observed in  $[\text{Pr}(\text{Ca},\text{Sr})\text{MnO}_3]$ ,<sup>20</sup> and Sr deficient samples  $\text{Pr}_{0.7}\text{Sr}_{0.3-x}\square_x\text{MnO}_3$ , where “ $\square$ ” means vacancy.<sup>21</sup> The lower and higher frequency lines around 100 and 605 MHz are ascribed to signals arising from FM domains or domain walls, since the spin-echo signal reduces rapidly when applying an external magnetic field. It was difficult to obtain the magnetic field dependence of resonance lines.

Here, we concentrate our attention on the NMR line observed around 320 MHz. This line has two peaks at 298 MHz and 318 MHz. The inset in Fig. 1 shows line shapes taken with different rf field  $H_1$ . The ratio of high rf power/low rf power is  $\sim 40$ , where the low rf power corresponds to  $\sim 1$  W of the output rf power from an amplifier. For a FM domain, the rf field acting in the nucleus is larger than the external rf fields  $H_1$  because of the strong rf enhancement created by the oscillating electron magnetic moment. On the other hand, NMR for AFM domains require higher rf power than that for FM domains, because of smaller rf enhancement. The line shape of  $\text{Bi}_{0.125}\text{Ca}_{0.875}\text{MnO}_3$  depends on rf power, which means that the signals arise from regions having different enhancement factors. The line shape taken with high rf power level has two peaks, whereas the one obtained with low rf power level has a single peak at  $\sim 318$  MHz.

Figure 2 shows the magnetic field dependence of the NMR line. The peak at 318 MHz in the higher frequency side decreases rapidly with increasing magnetic field. This behavior is consistent with the rf field dependence of the line shape shown in Fig. 1. The large signal enhancement is suppressed with the external magnetic field, which leads to the reduction in the signal intensity. Thus, the line appearing at 318 MHz in zero field is most likely associated to signals arising from a spin arrangement with FM component. These signals still appear in the frequency range 280–320 MHz, even under the field of 4 T. Assuming the line observed in external fields to consist of two Gaussians, we decomposed

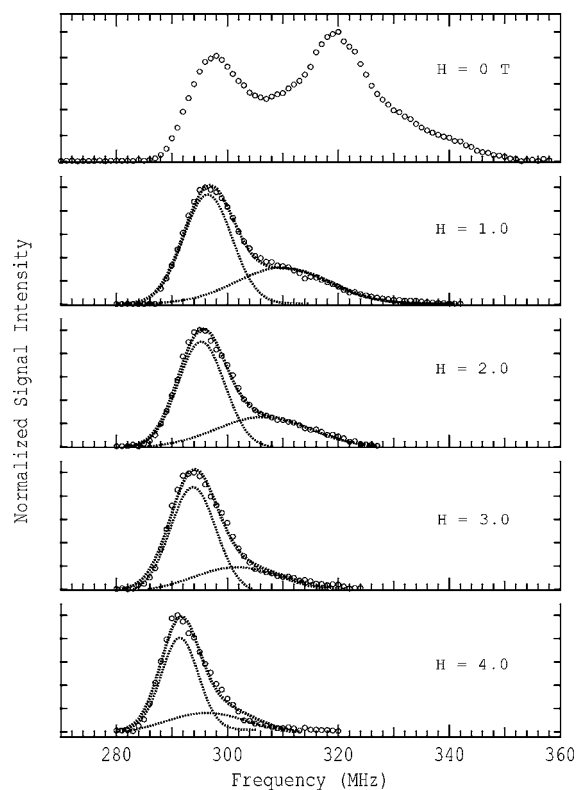


FIG. 2. External magnetic field dependence of NMR line taken at 4.2 K.

the line into upper and lower lines. These are shown with dotted lines in Fig. 2. The resonance frequencies of the upper and lower lines are plotted against the magnetic field in Fig. 3.

In the manganites, the spin-spin relaxation time,  $T_2$ , is often very short and frequency dependent.<sup>22</sup> We measured  $T_2$  at several points of the spectrum at 4.2 K in zero and 1 T magnetic fields. After correction for  $\tau \rightarrow 0$ , the spectrum shapes are almost the same as those without the correction, and the peak positions remain unchanged. Figure 4 shows the spin-echo amplitude decays taken at peak positions of the

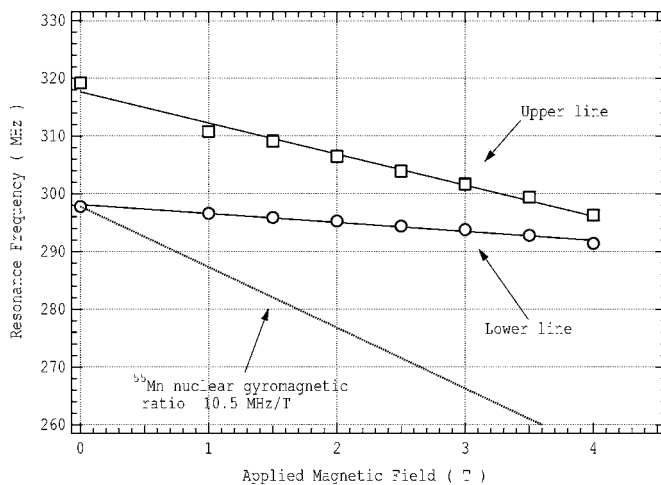


FIG. 3. The magnetic field dependences of the resonance frequencies of the upper and lower lines.

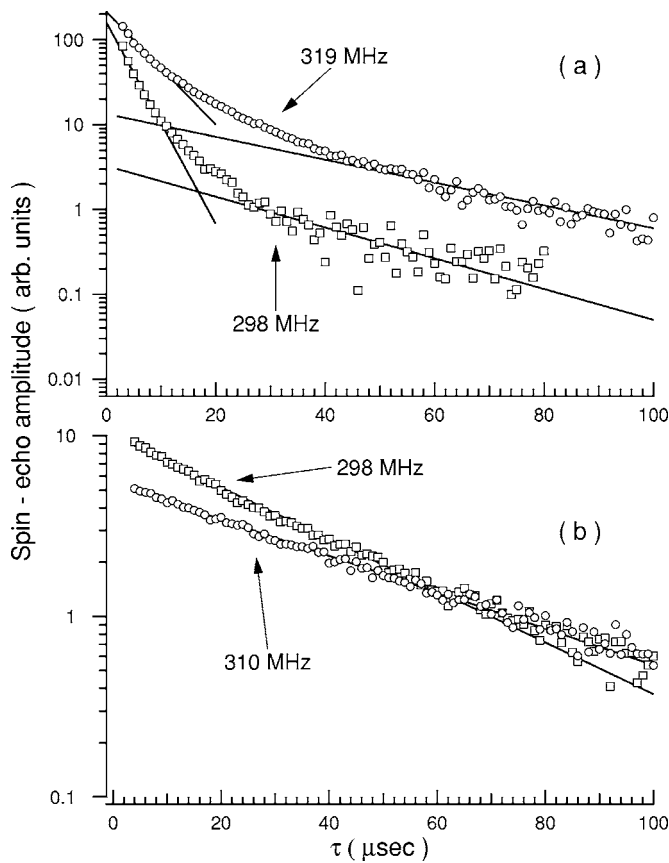


FIG. 4. The spin-echo amplitude decays at peak positions of spectra taken at 4.2 K (a) in zero-field and (b) in the field of 1 T.

lines. The decay curves taken in zero field are not single exponential, while the decays in the field of 1 T show single exponential behavior. The faster component may be attributed to the contribution of the FM domain walls.<sup>22</sup>

The lower line observed around 298 MHz shows a small shift in fields up to 4 T, with a rate of  $\sim -1.5$  MHz/T. The upper line shifts towards the low frequency side with a rate of  $\sim -5.4$  MHz/T. This rate is about one-half of that of the gyromagnetic ratio of <sup>55</sup>Mn, 10.5 MHz/T. The upper line does not shift according to the rate of the gyromagnetic ratio as expected for a collinear ferromagnet, although having FM signatures of large rf enhancement and magnetic field dependence of signal intensity. Thus, the frequency shift in external fields suggests that the upper line originates in a domain with a canted spin structure. The magnetization vs magnetic field taken at several temperatures are shown in Fig. 5. The magnetization is not saturated in the fields up to 7 T, and the maximum value is  $1.2\mu_B$  at 4.2 K. The results are in good agreement with those recently obtained by Woo *et al.*<sup>23</sup> which reveals no saturation in fields up to 30 T. The field dependence of NMR line around 320 MHz is consistent with the magnetization measurements results.

Figure 6 shows a temperature dependence of NMR line around 320 MHz. As temperature increased, the signal intensity of the upper line decreased rapidly, compared to that of the lower line. It was difficult to detect the signal corresponding to the upper line at temperatures above  $\sim 80$  K with our spectrometer. The reduction of the intensity of the

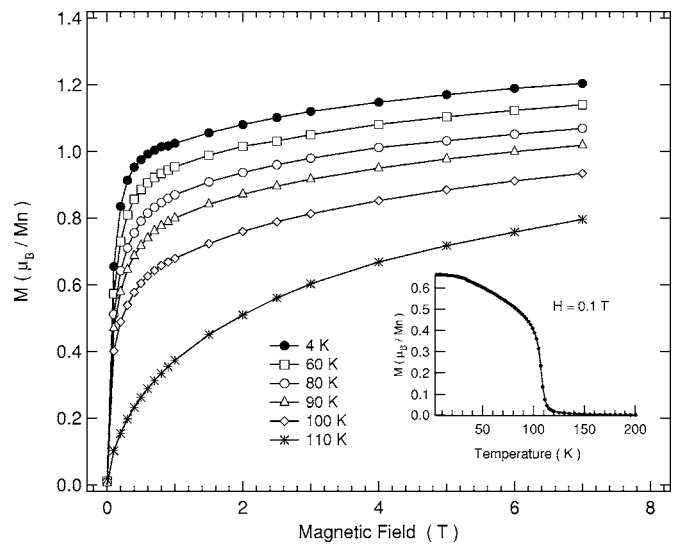


FIG. 5. Magnetization vs magnetic field at various temperatures. The inset shows the magnetization taken in 0.1 T.

upper line would be mainly connected with shortening of the spin-spin relaxation time  $T_2$ .

Figure 7 shows the temperature dependence of resonance frequencies of the upper and lower lines. The C-type spin structure, which exists up to about 100 K in

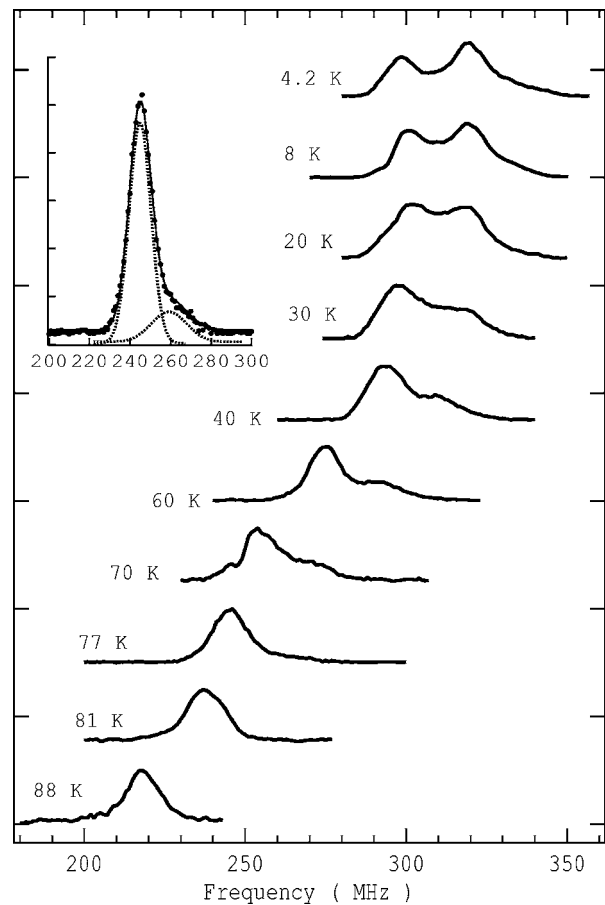


FIG. 6. Temperature dependence of resonance line. The inset shows the line taken at 77 K.

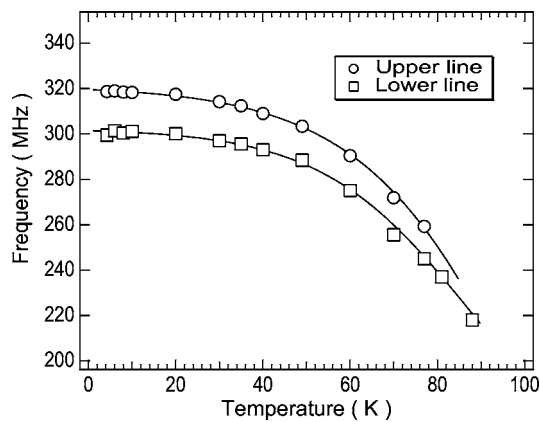


FIG. 7. The temperature dependences of the resonance frequencies of the upper and lower lines. The solid lines are guides for the eyes.

$\text{Bi}_{0.12}\text{Ca}_{0.88}\text{MnO}_3$ ,<sup>4</sup> consists of one-dimensional chains of parallel magnetic moments. The chains are aligned antiferromagnetically with each other. Substituting Bi for Ca dopes  $e_g$  electrons into the chain of the  $C$ -type AFM structure, which suggests double-exchange interactions along the chains. The magnetic moments which have been obtained for  $\text{Bi}_{0.12}\text{Ca}_{0.88}\text{MnO}_3$  from neutron diffraction measurements at low temperature are  $2.27\mu_B$  and  $2.52\mu_B$  for the  $G$ -type and  $C$ -type structures, respectively.<sup>4</sup> The majority phase is the  $G$ -type and the phase fraction is 87% at 20 K, while the fraction is 13% for the  $C$ -type phase. Thus, it is plausible that the lower NMR line observed for  $\text{Bi}_{0.125}\text{Ca}_{0.875}\text{MnO}_3$  is associated with Mn in the  $G$ -type structure, although we cannot determine the spin structure from the NMR results.

The resonance frequency of  $\text{CaMnO}_3$  is appreciably lower than that expected for  $\text{Mn}^{4+}$ , as shown in Fig. 1. Assuming the hyperfine coupling constant  $A$  for  $\text{Bi}_{0.125}\text{Ca}_{0.875}\text{MnO}_3$  to be the same as that for  $\text{CaMnO}_3$ , and corresponding the resonance frequency of 298 MHz to the magnetic moment of  $2.27\mu_B$ , we obtain the magnetic moment of  $\sim 2.0\mu_B/\text{Mn}$  in  $\text{CaMnO}_3$  from  $\nu=264$  MHz.

As was already mentioned for  $\text{Bi}_{0.125}\text{Ca}_{0.875}\text{MnO}_3$ , FM signals appear in the frequency range 60–160 MHz. It is worth noting that the hyperfine field of Mn in MnBi has been obtained to be 234.4 MHz at 77 K.<sup>24</sup> Therefore, the NMR line appearing in the frequency range 60–160 MHz for  $\text{Bi}_{0.125}\text{Ca}_{0.875}\text{MnO}_3$  is not attributed to signals from an impurity phase such as MnBi. Although we do not have a definite explanation for the appearance of the signals in the low frequency range, it might be due to the supertransferred hyperfine field through  $\text{Bi}^{3+}6s^2$  electrons. For electron doped manganites,  $\text{Ca}_{1-x}\text{R}_x\text{MnO}_3$  ( $R=\text{La,Pr}$ ), weak FM and AFM signals have been observed in the frequency range 200–280 MHz, together with strong FM signals around 300 MHz.<sup>19,22</sup> For  $\text{Bi}_{0.125}\text{Ca}_{0.875}\text{MnO}_3$ , however, the main line around 320 MHz arises from regions with AFM character. The observation of weak FM and strong AFM signals leads to the coexistence of minority FM region and majority AFM region. The field dependence of NMR lines suggests the AFM regions to be canted spin states.

In the present results, the NMR spectrum from  $\text{Mn}^{3+}$  has not been observed. The hyperfine coupling constant  $A$  of  $\text{Mn}^{3+}$  would be anisotropic because the  $\text{Mn}^{3+}$  is the Jahn-Teller ion. Consequently, the NMR spectrum of  $\text{Mn}^{3+}$  is broad and inhomogeneous.<sup>17</sup> Then, the  $\text{Mn}^{3+}$  spectrum is often practically smeared out.<sup>25,26</sup> Furthermore, signals arising from  $\text{Mn}^{2+}$  have been observed, which means that the charge disproportionation of the type,  $2\text{Mn}^{3+}$  into  $\text{Mn}^{2+}+\text{Mn}^{4+}$ , occurs in our sample. Thus, the recorded spectrum might indicate no  $\text{Mn}^{3+}$  signals because of the Jahn-Teller distortion and the charge disproportionation effects. It is difficult to determine amounts of  $\text{Mn}^{2+}$ , and of Mn ions observed in the low frequency range 60–160 MHz. Each have different signal enhancement factors.

#### ACKNOWLEDGMENTS

Sample preparation at NJIT was supported by NSF Grants Nos. DMR-0209243 and DMR-0512196.

\*Electronic address: shimizu@sci.u-toyama.ac.jp

<sup>1</sup>H. Chiba, M. Kikuchi, K. Kusaba, Y. Muraoka, and Y. Syono, *Solid State Commun.* **99**, 499 (1996).

<sup>2</sup>Wei Bao, J. D. Axe, C. H. Chen, and S.-W. Cheong, *Phys. Rev. Lett.* **78**, 543 (1997).

<sup>3</sup>H. L. Liu, S. L. Cooper, and S.-W. Cheong, *Phys. Rev. Lett.* **81**, 4684 (1998).

<sup>4</sup>P. N. Santhosh, J. Goldberger, P. M. Woodward, T. Vogt, W. P. Lee, and A. J. Epstein, *Phys. Rev. B* **62**, 14928 (2000).

<sup>5</sup>H. Woo, T. A. Tyson, M. Croft, S.-W. Cheong, and J. C. Woicik, *Phys. Rev. B* **63**, 134412 (2001).

<sup>6</sup>F. Sugawara, S. Iida, Y. Syono, and S. Akimoto, *J. Phys. Soc. Jpn.* **20**, 1529 (1965); **25**, 1553 (1968).

<sup>7</sup>E. O. Wollan and W. C. Koehler, *Phys. Rev.* **100**, 545 (1955).

<sup>8</sup>T. Atou, H. Chiba, K. Ohoyama, Y. Yamaguchi, and Y. Syono, *J. Solid State Chem.* **145**, 639 (1999).

<sup>9</sup>T. Kimura, S. Kawamoto, I. Yamada, M. Azuma, M. Takano, and

Y. Tokura, *Phys. Rev. B* **67**, 180401(R) (2003).

<sup>10</sup>A. Moreira dos Santos, A. K. Cheetham, T. Atou, Y. Syono, Y. Yamaguchi, K. Ohoyama, H. Chiba, and C. N. R. Rao, *Phys. Rev. B* **66**, 064425 (2002).

<sup>11</sup>Y. Murakami, D. Shindo, H. Chiba, M. Kikuchi, and Y. Syono, *Phys. Rev. B* **55**, 15043 (1997).

<sup>12</sup>M. Yu. Kagan, D. I. Khomskii, and M. V. Mostovoy, *Eur. Phys. J. B* **12**, 217 (1999).

<sup>13</sup>C. Martin, A. Maignan, M. Hervieu, B. Raveau, Z. Jirák, A. Kurbakov, V. Trounov, G. André, and F. Bourée, *J. Magn. Mater.* **205**, 184 (1999).

<sup>14</sup>C. D. Ling, E. Granado, J. J. Neumeier, J. W. Lynn, and D. N. Argyriou, *Phys. Rev. B* **68**, 134439 (2003); E. Granado, C. D. Ling, J. J. Neumeier, J. W. Lynn, and D. N. Argyriou, *ibid.* **68**, 134440 (2003).

<sup>15</sup>El'ad N. Caspi, M. Avdeev, S. Short, J. D. Jorgensen, M. V. Lobanov, Z. Zeng, M. Greenblatt, P. Thiyagarajan, C. E. Botez,

- and P. W. Stephens, Phys. Rev. B **69**, 104402 (2004).
- <sup>16</sup>G. Matsumoto, J. Phys. Soc. Jpn. **29**, 615 (1970).
- <sup>17</sup>A. Anane, C. Dupas, K. Le Dang, J. P. Renard, P. Veillet, A. M. de Leon Guevara, F. Millot, L. Pinsard, and A. Revcolevschi, J. Phys.: Condens. Matter **7**, 7015 (1995).
- <sup>18</sup>G. Allodi, R. De Renzi, G. Guidi, F. Licci, and M. W. Pieper, Phys. Rev. B **56**, 6036 (1997).
- <sup>19</sup>M. M. Savosta, P. Novák, M. Maryško, Z. Jiráček, J. Hejtmánek, J. Englich, J. Kohout, C. Martin, and B. Raveau, Phys. Rev. B **62**, 9532 (2000).
- <sup>20</sup>G. J. Tomka, P. C. Riedi, Cz. Kapusta, G. Balakrishnan, D. McK. Paul, M. R. Lees, and J. Barratt, J. Appl. Phys. **83**, 7151 (1998).
- <sup>21</sup>D. Abou-Ras, W. Boujelben, A. Cheikh-Rouhou, J. Pierre, J.-P. Renard, L. Reversat, and K. Shimizu, J. Magn. Magn. Mater. **233**, 147 (2001).
- <sup>22</sup>M. M. Savosta, P. Novák, J. Englich, J. Kohout, J. Hejtmánek, and A. Strejček, J. Magn. Magn. Mater. **242-245**, 676 (2002).
- <sup>23</sup>H. Woo, T. A. Tyson, M. Croft, and S-W. Cheong, J. Phys.: Condens. Matter **16**, 2689 (2004).
- <sup>24</sup>A. M. Portis and R. H. Lindqvist, in *Magnetism II A*, edited by G. T. Rado and H. Suhl (Academic, New York, 1965).
- <sup>25</sup>G. Papavassiliou, M. Fardis, M. Belesi, T. G. Maris, G. Kallias, M. Pissas, D. Niarchos, C. Dimitropoulos, and J. Dolinsek, Phys. Rev. Lett. **84**, 761 (2000).
- <sup>26</sup>Cz. Kapusta, P. C. Riedi, M. Sikora, and M. R. Ibarra, Phys. Rev. Lett. **84**, 4216 (2000).